Volume 54
Number 46
14 December 2025
Pages 16995-17348

Dalton Transactions

An international journal of inorganic chemistry

rsc.li/dalton

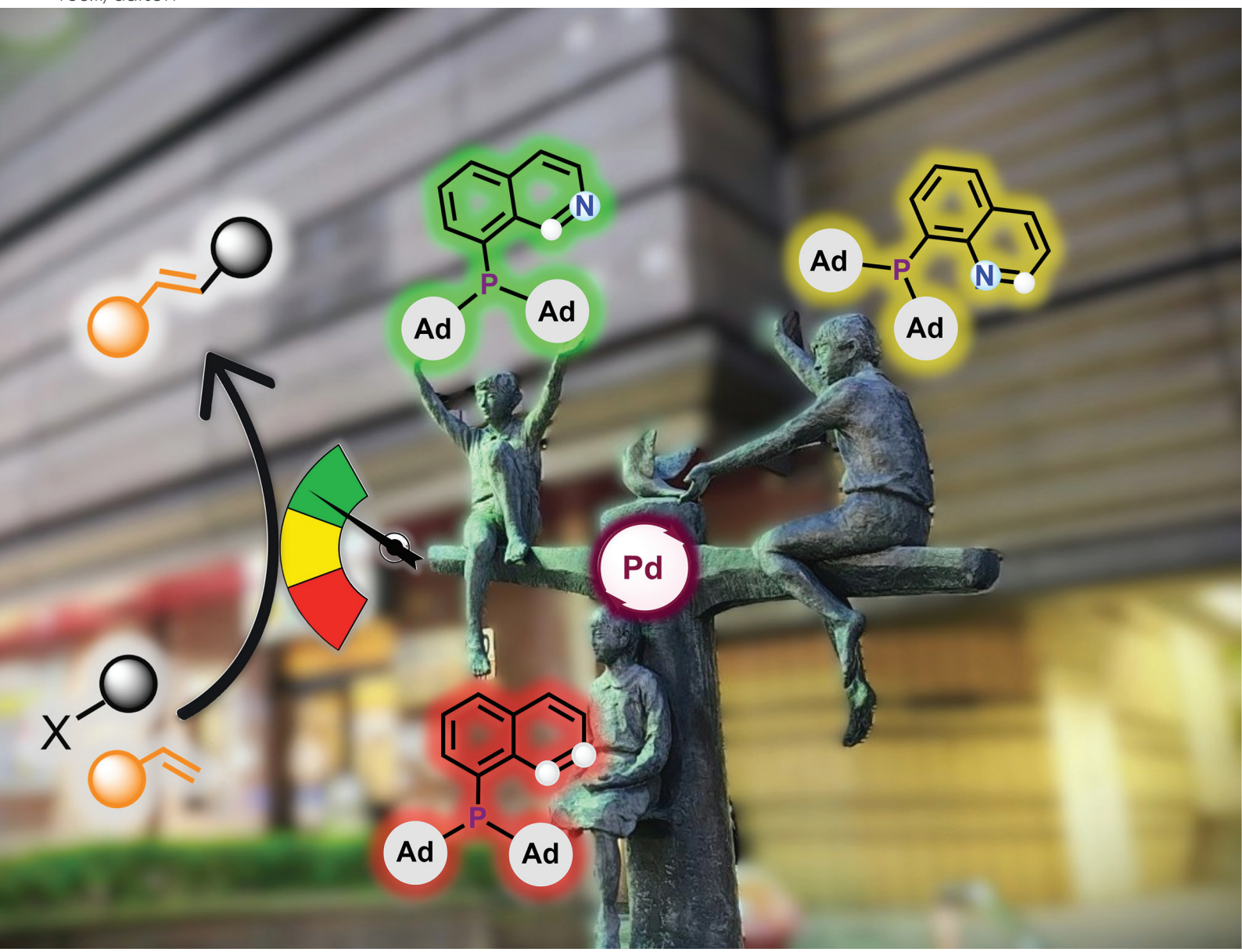

ISSN 1477-9226

ROYAL SOCIETY OF CHEMISTRY

COMMUNICATION

Chinraj Sivarajan and Raja Mitra

[Di(1-adamantyl)](aryl)phosphine ligands: synthesis, palladium complexation, and catalytic activity

Dalton Transactions

COMMUNICATION

View Article Online
View Journal | View Issue

Open Access Article. Published on 03 November 2025. Downloaded on 2/18/2026 12:40:07 PM.
This article is licensed under a Creative Commons Attribution-NonCommercial 3.0 Unported Licence.

Check for updates

Cite this: *Dalton Trans.*, 2025, **54**, 17073

Received 21st October 2025,
Accepted 29th October 2025

DOI: 10.1039/d5dt02523k

rsc.li/dalton

[Di(1-adamantyl)](aryl)phosphine ligands: synthesis, palladium complexation, and catalytic activity

Chinraj Sivarajan and Raja Mitra *

P(1-Ad)$_2$ (Ad = adamantyl) moiety-substituted quinoline, naphthyl, and isoquinoline ligands were synthesized to make Pd(II) complexes with κ^2-P^N/P^C coordination. Pd-based catalytic activity towards Mizoroki–Heck coupling of those phosphine ligands was examined, showing that the ligand *i*QAdPhos (L3) with an isoquinoline core possessing κ^2-P^C coordination was superior.

Ligand design and understanding its pivotal role in catalytic reactions is a fascinating field of organometallic chemistry, which keeps evolving.[1–3] The electronic nature and bulkiness of the substituent on the ligating site play a key role in tuning the catalytic activity, particularly for phosphine ligands.[4–7] Over time, the P^P ligand core[8–11] evolved into P^N or P^C type coordinating ligands, wherein N or C acts as a σ-donor.[12–29] The DalPhos class of ligands [P(1-Ad)$_2$(Ar); Ar = *o*-C$_6$H$_4$-NR$_2$] with phosphorus bearing bulky adamantyl (Ad) and P^N type coordination is crucial for C–N coupling using NH$_3$ (Fig. 1A).[28,29] Using the Dalphos ligand, catalytic systems with Pd[29] and Ni[30] were extensively studied by Stradiotto and coworkers. At the same time, (Dalphos)-Au complexes are being explored by Patil and coworkers in various alkene difunctionalization reactions,[31] suggesting the importance of P^N coordination where the N atom is sp^3 in nature. Interestingly, P^N coordination with an sp^2-type nitrogen is not extensively used for catalysis.[26,32,33] The quinoline core having PPh$_2$ or P(^{i}Pr)$_2$ at the 8th position resulted in κ^2-P^N coordinated metal complexes and their properties were studied (Fig. 1B).[12,34–37]

Metalation or deprotonation of a C–H bond in proximity to the phosphorus center led to the formation of P^C-coordinated Pd(II) complexes (Fig. 1C).[38–42] The κ^2-P^C ligated [P(Ph$_2$)(1-naphthyl)Pd(OAc)]$_2$ exhibited catalytic activity for the Mizoroki–Heck reaction,[43,44] affording 55% C–C coupled product (1 mol% catalyst; 130 °C; TOF = 61 h^{-1}).[38] For the isoquinoline core with PPh$_2$ substitution at the 8th position, the κ^2-P^C ligated Ru complex was synthesized, and its reactivity was studied (Fig. 1D);[45] however, the catalytic activity was not investigated. We envisage that changing the aromatic ring attached to the di(1-adamantyl)phosphine {P(1-Ad$_2$)} moiety might lead to controllable κ^2-P^N/P^C coordination towards Pd. Herein, we report P(1-Ad)$_2$ on quinoline, naphthyl, and isoquinoline cores as ligands, their coordination chemistry towards Pd, and their catalytic applications (Fig. 1E).

Following the literature,[46,47] di(1-adamantyl)phosphinic acid chloride was synthesized from adamantane using AlCl$_3$ and PCl$_3$, and it was further reduced using LiAlH$_4$ to obtain air-sensitive di(1-adamantyl)phosphine {(1-Ad)$_2$PH} (Fig. 2A).[47] The synthesized (1-Ad)$_2$PH was immediately used in Pd-catalyzed C–P coupling[47] with the corresponding aryl bromide to give the desired ligands (**L1–3**). 8-Bromoquinoline was used to synthesize 8-(di(1-adamantyl)phosphino)quinoline (QAdPhos; **L1**). 1-(Di(1-adamantyl)phosphino)naphthalene (NAdPhos; **L2**) was derived from 1-bromonaphthalene, and 8-(di(1-adaman-

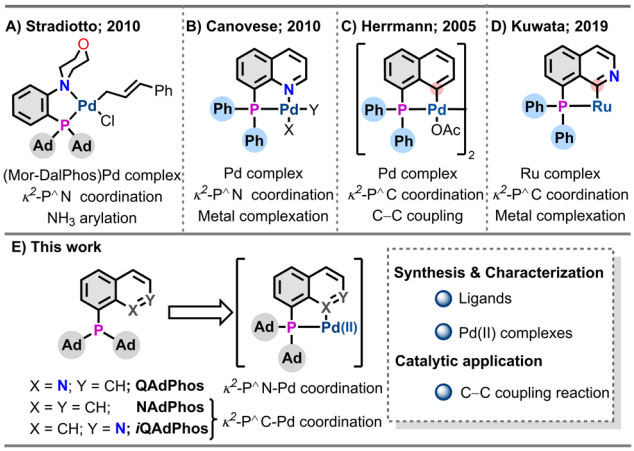

Fig. 1 (A) (Mor-DalPhos)Pd precatalyst. (B), (C) and (D) Previously reported PPh$_2$ analogue with an aromatic core showing a P^N/P^C coordination bound metal centre. (E) This work: P(1-Ad)$_2$ substituted ligand with an aromatic core and corresponding Pd complexes.

School of Chemical and Materials Sciences, Indian Institute of Technology Goa, Ponda, Goa-403401, India. E-mail: rajamitra@iitgoa.ac.in

Open Access Article. Published on 03 November 2025. Downloaded on 2/18/2026 12:40:07 PM.
This article is licensed under a Creative Commons Attribution-NonCommercial 3.0 Unported Licence.

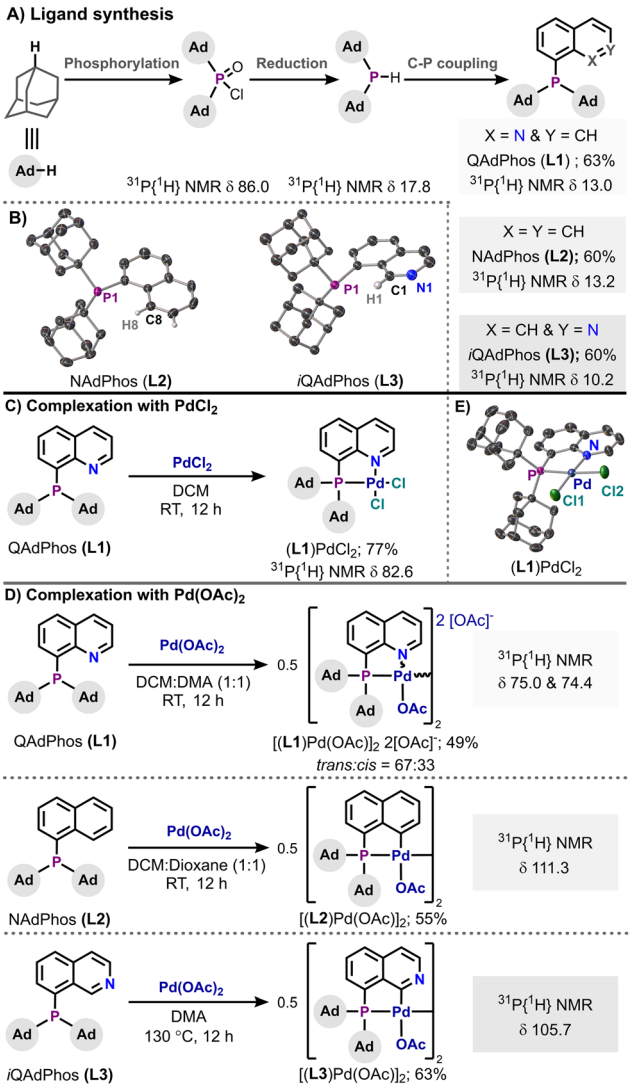

Fig. 2 (A) Synthesis of ligands (**L1–3**); $^{31}P\{^{1}H\}$ NMR spectra recorded in $CDCl_3$; δ in ppm. (B) Crystal structures of **L2** and **L3** (shown at a 50% probability of thermal ellipsoids; most of the H atoms are omitted for clarity). (C) and (D) Synthesis of Pd(II) complexes with **L1**, **L2**, and **L3**. (E) Crystal structure of the (**L1**)$PdCl_2{\cdot}3CH_2Cl_2$ complex (shown at a 50% probability of thermal ellipsoids; DCM solvents and H atoms are omitted for clarity). See the SI for details.

tyl)phosphino)isoquinoline (*i*QAdPhos; **L3**) was derived from 8-bromoisoquinoline (Fig. 2A).

$^{31}P\{^{1}H\}$ NMR showed a single peak of **L1** at 13.0 ppm, that of **L2** at 13.2 ppm, and that of **L3** at 10.2 ppm in $CDCl_3$. The P atom in these ligands was considerably shielded and electron-rich compared to Mor-Dalphos ($^{31}P\{^{1}H\}$ δ = 20.4 ppm)[28] and PAd_3 ($^{31}P\{^{1}H\}$ δ = 59.4 ppm).[48] The CH_2 (C_α from P) group in the 1-adamantyl moiety also showed a significant difference in the ^{1}H NMR spectra of all ligands, revealing the influence of nitrogen in proximity. The structures of **L2** and **L3** were further confirmed using single-crystal X-ray diffraction (scXRD),[49–51] which showed a distorted pyramidal geometry on the P atom (Fig. 2B). All three ligands were stable in the solid state and can be used on the benchtop. However, **L1** was sensitive to oxidation by air in the solution under ambient conditions (~9% oxidation after 48 h), whereas **L2** and **L3** were stable under the same conditions.

With the pure ligands, **L1–3**, in hand, we examined the complexation behavior with Pd(II). QAdPhos (**L1**) with $PdCl_2$ resulted in the expected κ^2-P^N coordinated (**L1**)$PdCl_2$ (Fig. 2C). The observed downfield shift in $^{31}P\{^{1}H\}$ NMR at δ 82.6 ppm confirmed the P^N coordination. The Pd complex was structurally characterized using scXRD (Fig. 2E). The bite angle of ∠PPdN was observed as 84.96° for (**L1**)$PdCl_2$, which was close to that reported for the (4-(2-(di(1-adamantyl)phosphino)phenyl)morpholine)Pd(η^1-1-phenylallyl) chloride complex (∠PPdN = 85.27°).[29] The reaction of $PdCl_2$ with **L2** and **L3** resulted in an uncharacterizable insoluble white solid, possibly a polymeric mixture.

The reaction of $Pd(OAc)_2$ with **L1** resulted in a P^N coordinated, μ-OAc bridged dimer with two OAc^- groups as counteranions {[(**L1**)Pd(OAc)]$_2$ 2[$OAc]^-$} (Fig. 2D). ATR-IR showed a broad band centered at 1603 cm^{-1} ($\nu_{C=O}$), and a sharp band at 1450 cm^{-1} (ν_{C-O}), which were consistent with the reported values for acetate.[52,53] The $^{31}P\{^{1}H\}$ NMR spectrum showed two peaks at 75.0 ppm (67%; *trans* isomer) and 74.4 ppm (33%; *cis* isomer). We speculate that the bulky Ad groups favor the *trans* isomer as the major isomer, as reported for the ^{t}Bu analog.[19,34] The *cis*:*trans* isomer ratio was also observed in ^{1}H and $^{13}C\{^{1}H\}$ NMR spectra. The ESI-MS analysis showed the $[C_{31}H_{39}PNO_2Pd]^+$ fragment *m*/*z* value of 594 (100%), corresponding to a partial dimer fragment. The reaction of $Pd(OAc)_2$ with **L2** resulted in a κ^2-P^C-coordinated dimer, [(**L2**)Pd(OAc)]$_2$ (55%), *via* acetate bridging without an additional base, which suggested that the OAc^- group acted as a base and facilitated P^C coordination (Fig. 2D). For [(**L2**)Pd(OAc)]$_2$, $^{31}P\{^{1}H\}$ NMR showed a peak at 111.3 ppm, and the H8 proton peak (δ = 9.16 ppm) of the ligand **L2** completely disappeared after Pd complexation, which confirmed the κ^2-P^C coordination (Fig. S3 & S4; SI). ESI-MS analysis showed a $[C_{30}H_{36}PPd]^+$ fragment *m*/*z* value of 533 (100%), which matched the P^C–Pd coordinated fragment. Under similar reaction conditions, **L3** did not proceed towards κ^2-P^C coordination as confirmed by $^{31}P\{^{1}H\}$ NMR. At higher temperature (130 °C) reaction of $Pd(OAC)_2$ with **L3** resulted in the κ^2-P^C coordinated complex [(**L3**)Pd(OAc)]$_2$. The dimer complex showed a peak at 105.7 ppm in $^{31}P\{^{1}H\}$ NMR, and the H1 proton peak (δ = 10.52 ppm) of the ligand **L3** completely disappeared after Pd complexation (Fig. S5 & S6; SI). ESI-MS showed a $[C_{62}H_{76}P_2N_2O_4Pd_2]^+$ corresponding peak at an *m*/*z* value of 1188 (100%) for the dimer [(**L3**)Pd(OAc)]$_2$. The ATR-IR spectra showed that peaks corresponding to acetates were consistent with the reported values.[52,53] All these characterization studies indicated the κ^2-P^N/P^C coordinated Pd dimer complex for all ligands.

Understanding Pd complex formation further motivated us to investigate the catalytic performance of these ligands. To explore the catalytic performance of **L1–3**, we began our study by focusing on the Mizoroki–Heck reaction (Table 1; Tables

 This journal is © The Royal Society of Chemistry 2025

Open Access Article. Published on 03 November 2025. Downloaded on 2/18/2026 12:40:07 PM.
This article is licensed under a Creative Commons Attribution-NonCommercial 3.0 Unported Licence.

Table 1 Reaction method development[a]

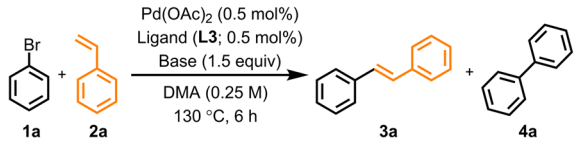

Entry	Conditions screened	3a (4a)[b]
1	**L1**; KOAc; 24 h	37 (5)
2	**L2**; KOAc; 24 h	19 (4)
3	**L3**; KOAc; 24 h	83 (7)
4	**L3**; $KHCO_3$; 24 h	93 (7)
5	**L3; $KHCO_3$; 6 h**	**95 (5)**
6[c]	0.25 mol% [(**L1**)Pd(OAc)]$_2$ 2[OAc]$^-$	47 (6)
7[c]	0.25 mol% [(**L2**)Pd(OAc)]$_2$	23 (2)
8[c]	0.25 mol% [(**L3**)Pd(OAc)]$_2$	93 (7)
9	PhI instead of PhBr	93 (7)
10	PhX (X = Cl, OTf, OTs) instead of PhBr	Not observed

[a] Optimized reaction conditions: bromobenzene (1 mmol), styrene (1.5 mmol), $Pd(OAc)_2$ (0.005 mmol), *i*QAdPhos/**L3** (0.005 mmol), and $KHCO_3$ (1.5 mmol) in degassed DMA (0.25 M) under argon. [b] GC conversions. [c] Only a Pd complex was used as a catalyst. See Tables S1–S11 in the SI.

S1–S11 in SI). 0.5 mol% of $Pd(OAc)_2$/**L3**, in the presence of KOAc in 0.25 M DMA, showed 83% **3a** and 7% **4a** after 24 h at 130 °C. Temperatures lower than 130 °C resulted in traces of **3a** (Table S4; SI). Among the Pd sources screened, $Pd(OAc)_2$ was found to be the most efficient (Table S5; SI). KOAc resulted in 83% **3a**; however, the milder base $KHCO_3$, a better alternative for hygroscopic KOAc, showed 93% **3a**. Other bases resulted in 2–80% conversion (Table S6, SI). Commercially available phosphine ligands like PPh_3 and 1,3-bis(diphenylphosphino) propane (dppp) showed 19–26% of **3a** under these conditions (Table S7, SI). Further decreasing the reaction time to 6 h gave 95% **3a** (TOF = 31.6 h^{-1}) and 5% **4a** (Table 1), as supported by the reaction profile obtained from gas chromatography (Fig. S7 and S8, SI). When the synthesized [(**L1**)Pd(OAc)]$_2$ 2[OAc]$^-$, [(**L2**)Pd(OAc)]$_2$, and [(**L3**)Pd(OAc)]$_2$ complexes were used as catalysts, they yielded 47%, 23% and 93% of **3a**, respectively, indicating that the ligand-coordinated Pd complex might be an active catalyst or pre-catalyst (Table 1). Reaction using 0.5 mol% $Pd(OAc)_2$ with 2, 3, and 5 equivalents of **L3** resulted in 21%, 8%, and <1% of **3a**, respectively, suggesting that bis-coordination deactivates the catalyst. Furthermore, it indicated that the Pd(II) to Pd(0) reduction might have occurred due to high temperature and the presence of $KHCO_3$ (Table S11, SI), not by phosphine ligand oxidation.[54,55] The reaction conditions were also compatible with aryl iodides, yielding conversions comparable to those of aryl bromides (Table 1). Aryl chloride and aryl pseudohalides failed to react under the optimized conditions (Table 1). The control reactions revealed that all reactants and catalysts were necessary to obtain product **3a**. Without **L3**, only 12% **3a** was observed, supporting the ligand-controlled catalytic cycle (SI).

The optimized conditions were further explored for various substrates bearing electronic and steric factors (Fig. 3). Bromobenzene resulted in 89% (TOF = 29.6 h^{-1}; 6 h) isolated yield of *E*-stilbene (**3a**) and 85% isolated yield for a large-scale reaction (5 mmol, 0.785 g) using 0.1 mol% catalyst loading (TOF = 141.9 h^{-1}; 30 h). Electron-donating substituents, such

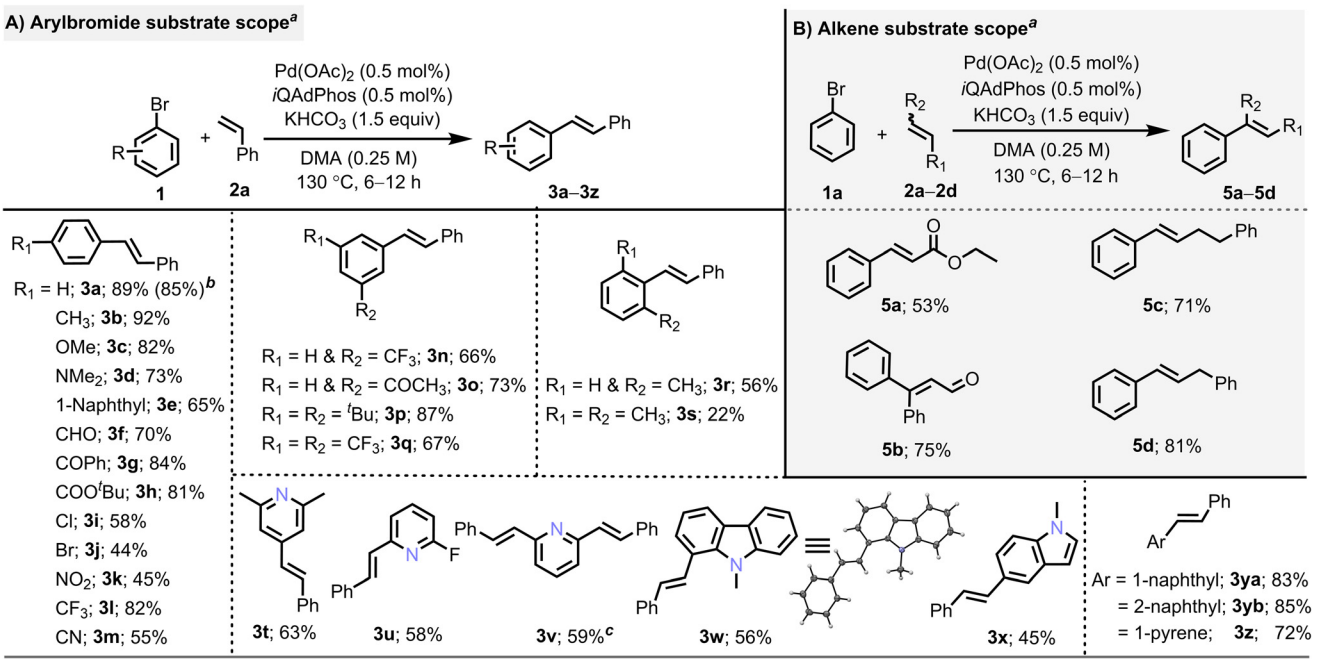

Fig. 3 Substrate scope. [a] Reaction conditions: aryl bromide (1 mmol), alkene (1.5 mmol), $Pd(OAc)_2$ (0.005 mmol), *i*QAdPhos (0.005 mmol), and $KHCO_3$ (1.5 mmol) in degassed DMA (0.25 M) for 6–12 h at 130 °C under argon. The reported isolated yields are the average of at least two reactions. [b] 5 mmol PhBr reaction scale using a 0.1 mol% catalyst loading for 30 h and [c] 5 equivalents of styrene and $KHCO_3$ were used.

Open Access Article. Published on 03 November 2025. Downloaded on 2/18/2026 12:40:07 PM. This article is licensed under a Creative Commons Attribution-NonCommercial 3.0 Unported Licence.

as *p*-Me (**3b**), *p*-OMe (**3c**), *p*-NMe_2(**3d**), and *p*-1-naphthyl (**3e**), resulted in 65–92% yields. They were also suitable for various reactive functional groups, such as *p*-CHO (**3f**; 70%), *p*-COPh (**3g**; 84%), and *p*-COO^tBu (**3h**; 81%). The halogen substituents, *p*-Cl and *p*-Br, resulted in 58% (**3i**) and 44% (**3j**) yields, respectively, with the retention of one Cl and Br. EWGs, such as *p*-NO_2 (**3k**), *p*-CF_3 (**3l**), and *p*-CN (**3m**), yielded the desired products (45–82%). *m* and *m*,*m*′ substituted derivatives such as **3n** (66%), **3o** (73%), **3p** (87%), and **3q** (67%) were obtained in good yields. *o*-Me (**3r**; 56%) and *o*,*o*′-Me (**3s**; 22%) furnished moderate yields, probably due to steric reasons. The pyridine heterocycles also worked well under these conditions, resulting in **3t** (63%), **3u** (58%), and **3v** (59%). 1-Bromo-9-methyl-9*H*-carbazole and 5-bromo-1-methyl-1*H*-indole yielded 56% (**3w**; structurally characterized) and 45% (**3x**) of the desired product, respectively. 1-Bromonaphthalene, 2-bromonaphthalene, and 1-bromopyrene substrates gave good yields of **3ya** (83%), **3yb** (85%), and **3z** (72%), respectively. The α,β-unsaturated carbonyl derivatives were tolerated under the optimized reaction conditions and yielded the desired *E* product in 53% (**5a**) and 75% (**5b**) yields. Allylbenzene and 4-phenyl-1-butene also gave 71% (**5c**) and 81% (**5d**) yields of the major products with a minor geminal isomer as observed in ^{1}H NMR spectra (<10%; SI). We found that a few substrates (unactivated olefins, reactive heterocycles, *etc*.) showed either complex or no reactivity (SI).

In conclusion, we synthesized a series of bulky di(1-adamantyl)(aryl)phosphine {$P(1\text{-Ad})_2(Ar)$} ligands, **L1–3**, featuring quinoline, naphthyl, and isoquinoline substituents, enabling the formation of Pd(II) complexes that coordinate through κ^2-P^N and P^C modes. Among these, the ligand *i*QAdPhos (**L3**) showed excellent catalytic activity with 0.5 mol% $Pd(OAc)_2$ (TOF = 29.6 h^{-1}). The catalyst loading could be further reduced to 0.1 mol% by extending the time (TOF = 141.9 h^{-1}). We tested a variety of (hetero)aryl bromides and alkenes, achieving moderate to excellent yields of the Mizoroki–Heck coupling products (22–92% isolated yields). This study demonstrates the potential of bulky $P(1\text{-Ad})_2(Ar)$ ligands in Pd-catalyzed C–C bond formation and offers valuable insights into ligand design and Pd coordination.

Conflicts of interest

There are no conflicts to declare.

Data availability

Supplementary information (SI): experimental and spectral data. See DOI: https://doi.org/10.1039/d5dt02523k.

CCDC 2469531 (**L2**), 2469533 (**L3**), 2469538 ((**L1**)$PdCl_2{\cdot}3CH_2Cl_2$) and 2495634 (**3w**) contain the supplementary crystallographic data for this paper.[56a–d]

Acknowledgements

All authors thank the Indian Institute of Technology Goa (IIT Goa) for the infrastructure and Max-Planck-Gesellschaft (MPG) and Max-Planck-Institut für Kohlenforschung (MPI Kofo) for the generous funding through the "Max Planck India partner group" project. We are grateful to Prof. Benjamin List for his support throughout this project. We thank Ms. Nikita G. and Prof. Sunder N. Dhuri, Goa University, and Mr. Sivaraj Chandrasekaran, VIT, Chennai, for the scXRD data.

References

1 D. S. Surry and S. L. Buchwald, *Chem. Sci.*, 2010, **2**, 27–50.
2 L.-C. Campeau and N. Hazari, *Organometallics*, 2019, **38**, 3–35.
3 P. G. Gildner and T. J. Colacot, *Organometallics*, 2015, **34**, 5497–5508.
4 T. L. Brown and K. J. Lee, *Coord. Chem. Rev.*, 1993, **128**, 89–116.
5 M. Kranenburg, P. C. J. Kamer, P. W. N. M. van Leeuwen, D. Vogt and W. Keim, *J. Chem. Soc., Chem. Commun.*, 1995, 2177–2178.
6 C. A. Tolman, *Chem. Rev.*, 1977, **77**, 313–348.
7 Z. Freixa and P. W. N. M. van Leeuwen, *Dalton Trans.*, 2003, 1890–1901.
8 J. F. Hartwig, *Inorg. Chem.*, 2007, **46**, 1936–1947.
9 D. S. Surry and S. L. Buchwald, *Angew. Chem., Int. Ed.*, 2008, **47**, 6338–6361.
10 H.-J. Xu, Y.-Q. Zhao and X.-F. Zhou, *J. Org. Chem.*, 2011, **76**, 8036–8041.
11 C. Sivarajan, S. Saha, S. Mulla and R. Mitra, *J. Org. Chem.*, 2024, **89**, 17021–17030.
12 P. Schiltz, N. Casaretto, S. Bourcier, A. Auffrant and C. Gosmini, *Dalton Trans.*, 2023, **52**, 14859–14866.
13 J. James, M. Jackson and P. J. Guiry, *Adv. Synth. Catal.*, 2019, **361**, 3016–3049.
14 P. J. Guiry and C. P. Saunders, *Adv. Synth. Catal.*, 2004, **346**, 497–537.
15 H. A. Hudali, J. V. Kingston and H. A. Tayim, *Inorg. Chem.*, 1979, **18**, 1391–1394.
16 G. Sabharwal, K. C. Dwivedi and M. S. Balakrishna, *Dalton Trans.*, 2025, **54**, 11551–11562.
17 J. Monot, E. Marelli, B. Martin-Vaca and D. Bourissou, *Chem. Soc. Rev.*, 2023, **52**, 3543–3566.
18 J. Dupont, C. S. Consorti and J. Spencer, *Chem. Rev.*, 2005, **105**, 2527–2572.
19 W. A. Herrmann, C. Brossmer, C.-P. Reisinger, T. H. Riermeier, K. Öfele and M. Beller, *Chem. – Eur. J.*, 1997, **3**, 1357–1364.
20 F. Schroeter, J. Soellner and T. Strassner, *ACS Catal.*, 2017, **7**, 3004–3009.
21 L. Canovese, C. Santo and F. Visentin, *Organometallics*, 2008, **27**, 3577–3581.
22 T. Tsukuda, C. Nishigata, K. Arai and T. Tsubomura, *Polyhedron*, 2009, **28**, 7–12.
23 T. Suzuki, *Bull. Chem. Soc. Jpn.*, 2004, **77**, 1869–1876.

 This journal is © The Royal Society of Chemistry 2025

Open Access Article. Published on 03 November 2025. Downloaded on 2/18/2026 12:40:07 PM. This article is licensed under a Creative Commons Attribution-NonCommercial 3.0 Unported Licence.

24 Y. Canac, *Chem. Rec.*, 2023, **23**, e202300187.
25 J. James and P. J. Guiry, *ACS Catal.*, 2017, **7**, 1397–1402.
26 S. Jin, L. Liu and F. Lin, *Organometallics*, 2025, **44**, 2025–2034.
27 R. J. Lundgren, K. D. Hesp and M. Stradiotto, *Synlett*, 2011, 2443–2458.
28 R. J. Lundgren, B. D. Peters, P. G. Alsabeh and M. Stradiotto, *Angew. Chem., Int. Ed.*, 2010, **49**, 4071–4074.
29 P. G. Alsabeh, R. J. Lundgren, R. McDonald, C. C. C. Johansson Seechurn, T. J. Colacot and M. Stradiotto, *Chem. – Eur. J.*, 2013, **19**, 2131–2141.
30 K. M. Morrison and M. Stradiotto, *Chem. Sci.*, 2024, **15**, 7394–7407.
31 A. B. Gade, Urvashi and N. T. Patil, *Org. Chem. Front.*, 2024, **11**, 1858–1895.
32 P. Schiltz, N. Casaretto, A. Auffrant and C. Gosmini, *Chem. – Eur. J.*, 2022, **28**, e202200437.
33 S. Kelly, R. Goddard and P. J. Guiry, *Helv. Chim. Acta*, 2022, **105**, e202100205.
34 L. Canovese, F. Visentin, G. Chessa, C. Santo and A. Dolmella, *Dalton Trans.*, 2009, 9475–9485.
35 L. Canovese, F. Visentin, T. Scattolin, C. Santo and V. Bertolasi, *Dalton Trans.*, 2015, **44**, 15049–15058.
36 T. Scattolin, F. Visentin, C. Santo, V. Bertolasi and L. Canovese, *Dalton Trans.*, 2017, **46**, 5210–5217.
37 T. Suzuki, H. Yamaguchi, M. Fujiki, A. Hashimoto and H. D. Takagi, *Acta Crystallogr., Sect. E:Crystallogr. Commun.*, 2015, **71**, 447–451.
38 G. D. Frey, C.-P. Reisinger, E. Herdtweck and W. A. Herrmann, *J. Organomet. Chem.*, 2005, **690**, 3193–3201.
39 C. Amatore and A. Jutand, *Acc. Chem. Res.*, 2000, **33**, 314–321.
40 B. L. Shaw, *Chem. Commun.*, 1998, 1361–1362.
41 M. Beller, H. Fischer, W. A. Herrmann, K. Öfele and C. Brossmer, *Angew. Chem., Int. Ed. Engl.*, 1995, **34**, 1848–1849.
42 W. A. Herrmann, C. Brossmer, K. Öfele, C.-P. Reisinger, T. Priermeier, M. Beller and H. Fischer, *Angew. Chem., Int. Ed. Engl.*, 1995, **34**, 1844–1848.
43 T. Mizoroki, K. Mori and A. Ozaki, *Bull. Chem. Soc. Jpn.*, 1971, **44**, 581.
44 R. F. Heck and J. P. Nolley Jr., *J. Org. Chem.*, 1972, **37**, 2320–2322.
45 N. Tashima, T. Sawazaki, Y. Kayaki and S. Kuwata, *Chem. Lett.*, 2019, **48**, 787–790.
46 J. R. Goerlich and R. Schmutzler, *Phosphorus, Sulfur Silicon Relat. Elem.*, 1995, **102**, 211–215.
47 Á. Sinai, D. C. Simkó, F. Szabó, A. Paczal, T. Gáti, A. Bényei, Z. Novák and A. Kotschy, *Eur. J. Org. Chem.*, 2020, 1122–1128.
48 L. Chen, P. Ren and B. P. Carrow, *J. Am. Chem. Soc.*, 2016, **138**, 6392–6395.
49 O. V. Dolomanov, L. J. Bourhis, R. J. Gildea, J. A. K. Howard and H. Puschmann, *J. Appl. Crystallogr.*, 2009, **42**, 339–341.
50 G. M. Sheldrick, *Acta Crystallogr., Sect. A:Found. Adv.*, 2008, **64**, 112–122.
51 G. M. Sheldrick, *Acta Crystallogr., Sect. A:Found. Crystallogr.*, 2015, **71**, 3–8.
52 E. Spinner, *J. Chem. Soc.*, 1964, 4217–4226.
53 F. Villalba, S. Martín-Martín and A. C. Albéniz, *ChemCatChem*, 2025, e00335.
54 T. Fantoni, C. Palladino, R. Grigolato, B. Muzzi, L. Ferrazzano, A. Tolomelli and W. Cabri, *Org. Chem. Front.*, 2025, **12**, 1982–1991.
55 F. d'Orlyé and A. Jutand, *Tetrahedron*, 2005, **61**, 9670–9678.
56 (*a*) CCDC 2469531: Experimental Crystal Structure Determination, 2025, DOI: 10.5517/ccdc.csd.cc2nwr9m; (*b*) CCDC 2469533: Experimental Crystal Structure Determination, 2025, DOI: 10.5517/ccdc.csd.cc2nwrcp; (*c*) CCDC 2469538: Experimental Crystal Structure Determination, 2025, DOI: 10.5517/ccdc.csd.cc2nwrjv; (*d*) CCDC 2495634: Experimental Crystal Structure Determination, 2025, DOI: 10.5517/ccdc.csd.cc2prxbq.